



Published in final edited form as:

Nat Mater. 2019 March ; 18(3): 289–297. doi:10.1038/s41563-018-0271-6.

Sterile particle induced inflammation is mediated by macrophages releasing IL-33 through a Bruton's tyrosine kinase-dependent pathway

Pankaj K. Mishra^{1,2,*}, Mark Palma^{1,2,*}, Bonnie Buechel³, Jeffrey Moore⁴, Viralkumar Davra⁵, Niansheng Chu⁶, Ariel Millman^{1,2}, Nadim J. Hallab⁷, Thirumala-Devi Kanneganti⁸, Raymond B. Birge⁵, Edward M. Behrens⁶, Amariliz Rivera², Kathleen S. Beebe^{2,3}, Joseph Benevenia³, and William C. Gause^{1,2}

¹Department of Medicine, Rutgers – New Jersey Medical School, Newark, NJ, 07103;

²Center for Immunity and Inflammation, Rutgers – New Jersey Medical School, Newark, NJ, 07103;

³Department of Orthopaedic Surgery, Rutgers – New Jersey Medical School, Newark, NJ, 07103

⁴Department of Orthopaedic Surgery, Seton Hall University – St. Joseph's Regional Medical Center, Paterson, NJ, 07503

⁵Department of Microbiology, Biochemistry and Molecular Genetics, Cancer Center, Rutgers – New Jersey Medical School, Newark, NJ, 07103

⁶Division of Pediatric Rheumatology, Children's Hospital of Philadelphia, Philadelphia, PA, 19104

⁷Department of Orthopaedic Surgery, Rush University Medical Center, Chicago, IL, 60612

⁸Department of Immunology, St. Jude Children's Research Hospital, Memphis, TN, 38105-3678;

Abstract

Initiation of the innate sterile inflammatory response that can develop in response to microparticle (MP) exposure is little understood. A potent type 2 immune response associated with accumulation of neutrophils, eosinophils, and alternatively activated (M2) macrophages was observed in response to sterile MPs similar in size to wear debris associated with prosthetic implants. Although elevations in IL-33 and type 2 cytokines occurred independently of Caspase-1

Correspondence should be addressed to W.C.G (gausewc@njms.rutgers.edu).

Author's contributions

WCG, PKM, MP, and KB designed the experiments. PKM and MP conducted all the experiments. BB and JM helped in collecting and processing of tissue biopsies from human clinical samples and AM provided technical assistance with immune staining. NJH determined the sizes of wear debris particles and helped in particle separation. TK provided Caspase1^{-/-} mice and technical suggestions for the experiments. KB and JB coordinated the clinical studies with human subjects. VD and RB provided technical assistance and advice in experiments assessing macrophage death and phagocytosis. CN and EB provided ST2^{-/-} mice, laboratory assistance and suggestions for the experiments. AR provided the CCR2 reporter mice and associated technical assistance. WCG, PKM, and MP wrote this manuscript.

*Authors Contributed Equally.

Competing Financial Interests

The authors declare no competing financial interests.

Data Availability Statement

The data that support the findings of this study are available from the corresponding author upon reasonable request

inflammasome signaling, the response was dependent on Bruton's tyrosine kinase (BTK). IL-33 was produced by macrophages and BTK-dependent expression of IL-33 by macrophages was sufficient to initiate the type 2 response. Analysis of inflammation in patient periprosthetic tissue also revealed type 2 responses under aseptic conditions in patients undergoing revision surgery. These findings indicate for the that MP-induced sterile inflammation is initiated by macrophages activated to produce IL-33. They further suggest that both BTK and IL-33 may provide therapeutic targets for wear debris induced periprosthetic inflammation.

Introduction:

Prosthetic implants for joint reconstruction are widely used; however, as many as 15% of joint replacements will fail, often requiring revision surgery¹. The major cause is likely microparticles (MPs) released from prosthetic devices, commonly referred to as wear debris, that are thought to promote localized sterile inflammation leading to pain, osteolysis, loosening of the implant and ultimately failure of fixation. The immune signaling pathways through which these apparently inert solid MPs promote such harmful inflammation remain unclear and their characterization may reveal new targets for the development of effective therapies^{2, 3, 4}. As macrophages are often associated with wear debris in periprosthetic tissue, these myeloid cells have been proposed to be essential players⁵. Also, in vitro cultures have indicated that wear debris can promote macrophage activation and inflammatory cytokine production, including TNF-alpha and IL-1beta^{2, 6}, with a number of reports concluding that MPs similar to wear debris may trigger type 1 immune responses. However, this remains controversial as the presence of endotoxin in some MP preparations or in infection associated implants may skew the response^{7, 8, 9}, obscuring sterile responses associated with the MPs themselves.

We have previously reported that endotoxin-free MPs, similar in size to wear-debris particles, also induce a type 2 innate response with increases in M2 macrophages, neutrophils, and eosinophils through TLR-4-independent pathways¹⁰. These findings are consistent with studies of other sterile particulate inert structures, including monosodium urate (MSU) crystals¹¹ and silica¹², where type 2 immune responses were also observed. In the present study, we now interrogate the mechanisms that initiate innate sterile type 2 inflammation induced by metallic MPs of a similar size and composition to wear debris particles. Our studies reported herein indicate that BTK signaling specifically upregulates macrophage production of IL-33, which is required for the initiation of the MP induced type 2 immune response. These studies thus indicate a critical role for IL-33 producing macrophages in driving the initiation of the sterile inflammatory response to inert particulates.

Results and Discussion

MPs induce a Caspase 1-independent type 2 innate response

We have reported that micrometer sized titanium (Ti) particles, similar in size to wear debris particles associated with prosthetic implants, induce a robust type 2 innate response independently of TLR-4 by 48 hours after inoculation¹⁰. To assess whether this response

was characteristic of micrometer sized metallic particles generally, C57BL/6 (BL/6) mice were inoculated intra-peritoneally (i.p.) with either vehicle or similarly sized solid inert cobalt chrome alloy MPs (0.3–100 μ m), which is a commonly used implant material² and is used in all experiments described in this manuscript. At 2 days after MP inoculation, peritoneal exudate cells (PECs) were analyzed for innate immune cell markers. Neutrophils (CD11b⁺, Ly6G⁺), eosinophils (c-Kit⁻, Siglec-F⁺), and M2 macrophages (F4/80⁺, CD206⁺) were increased (Supplementary Figure 1A, B) following MP inoculation. Gene expression analysis showed that type 2 cytokines (Il-4, Il-5, Il-13), alternatively activated (M2) macrophage markers (Arg1, Retnla, Chi3l3), cytokine alarmins (Il-25 and Il-33), and the type 2 associated NOTCH ligand, Jag-1, were all upregulated in PECs exposed to MPs. In contrast, genes associated with innate type 1 or type 17 responses (Il-12, Inos, Delta4, and Il-17) were not increased, indicating polarization towards a type 2 immune response (Supplementary Figure 1C) as early as day 2 after inoculation. Interestingly, modest increases in IFN- γ were also detected, likely derived from natural killer or other innate lymphoid cells.

To assess whether the Caspase-1 dependent inflammasome might contribute to MP-induced inflammation, Caspase-1^{-/-} mice were inoculated with MPs. Increases in eosinophils and M2 macrophages were intact; however, decreases in neutrophils were evident in Caspase-1^{-/-} mice when compared to inoculated WT controls (Supplementary Figure 1A, B). Intriguingly, similar increases in type 2 cytokines were observed in Caspase-1^{-/-} mice (Supplementary Figure 1C). Although Caspase-1 generally promotes functional IL-1 β activity¹³, increases in Caspase-1 independent IL-1 β have also been described in response to *Mycobacterium tuberculosis* infection¹⁴. However, our findings showed that IL-1 β elevations were blocked in MP-inoculated Caspase-1^{-/-} mice, as shown in Supplementary Figure 1D. In a separate experiment, using CC chemokine receptor 2 (CCR2) reporter mice, approximately 40% of the peritoneal macrophages were CCR2⁺ at 2 days after MP inoculation, indicating they were blood monocyte-derived (Supplementary Figure 1E). The MP mediated innate immune response was sufficiently robust to function as an adjuvant that could prime *in vivo* Ag-specific DO11.10 Th2 cell differentiation (Supplementary Figure 2). Taken together, these findings indicated that blockade of the Caspase-1 dependent inflammasome has little effect on the potent type 2 innate immune response to sterile inert MPs.

The MP-induced type 2 response is SYK dependent

In vitro studies have implicated the spleen tyrosine kinase (SYK) pathway in particulate induced inflammation, triggered through receptor independent cell membrane perturbations associated with frustrated phagocytosis^{15, 16}. Furthermore, inhibition of SYK signaling can block Ag-specific serum IgE elevations following OVA-alum immunization¹². To interrogate the role of SYK in MP-induced inflammation, we administered Bay 61–3606, a potent and selective SYK inhibitor¹⁷. Mice were orally gavaged with either Bay 61–3606 or vehicle twice per day starting 2 days prior to i.p. MP inoculation. At day 2 after MP inoculation, peritoneal cells were analyzed for immune cell phenotypes by FACS analysis and cytokine gene expression by qPCR. MP inoculated mice administered Bay 61–3606 showed marked reductions in neutrophils, eosinophils, and M2 macrophages. Decreases in PEC type 2

cytokines, including IL-4, IL-5, and IL-13 mRNA, were also observed. In addition, MP-induced elevations in the cytokine alarmin, IL-33, known to trigger type 2 responses¹⁸, were also blocked, as measured by PEC IL-33 mRNA and peritoneal fluid (PF) protein levels (Supplementary Figure 3A–D). PECs from MP-inoculated mice also showed elevations of activated pSYK (Y348), which was blocked by Bay 61–3606 (Supplementary Figure 3E). As Bruton's tyrosine kinase (BTK) signaling can be SYK-dependent¹⁹, we also measured BTK phosphorylation. Enhanced PEC BTK phosphorylation was blocked by administration of Bay 61–3606 (Supplementary Figure 3F). Thus, SYK inhibition generally inhibited immune cell infiltration and elevations in IL-33 and type 2 cytokines.

BTK drives type 2 inflammation independently of B cells

SYK signaling involves multiple downstream pathways, including BTK activation (Y551)²⁰. To specifically examine the role of the BTK pathway, we used Ibrutinib, which irreversibly inhibits BTK^{21, 22, 23}. Neutrophils, eosinophils, and M2 macrophages, were reduced in MP inoculated groups treated with Ibrutinib. BTK blockade also inhibited M2 marker, type 2 cytokine, and IL-33 mRNA, PF IL-33 protein, and activated pBTK (Y551). However, Ibrutinib administration did not alter MP mediated activation of pSYK (Y348), consistent with its activation being downstream of SYK signaling (Supplementary Figure 4). Thus, Ibrutinib inhibited immune cell infiltration and elevations in type 2 cytokines and IL-33.

As BTK is associated with B cell activation and Ab-mediated signaling in innate immune cell populations¹⁹, we next examined whether B cells were required for MP-induced inflammation. BALB/c control mice or B cell deficient $Jh^{-/-}$ mice were inoculated with MPs, assessed at 48 hours, and inflammation was similar in both strains [Supplementary Figure 5 (A–C)], indicating that MP-induced inflammation is independent of B cells. B cells were undetectable in $Jh^{-/-}$ mice (Supplementary Figure 5D). As Ibrutinib can also block T cell receptor (TCR) interleukin-2 inducible kinase (ITK) signaling²⁴, we depleted T cells with an anti-CD4 (GK1.5) Ab, as described previously²⁵, and inoculated mice i.p. with MPs. CD4 T cell depletion had no effect on the MP-induced immune response (Supplementary Figure 6A–C). Thus, neither B cells nor T cells are essential for this BTK-dependent MP-induced type 2 response.

To further investigate the role of BTK signaling in this innate inflammatory response, we utilized mutant CBA/N^{xid} (BTK deficient) mice, which have a BTK loss of function mutation^{26, 27}. CBA/CaJ wild type or BTK deficient mice were inoculated i.p. with either vehicle (PBS) or MPs. As shown in Figure 1 (A–B), MP-induced increases in innate immune cell populations were blocked in BTK functional knockouts compared to inoculated wild type mice. Gene expression of IL-33, type 2 cytokines and markers for M2 macrophages were also decreased (Figure 1C). Although constitutive loss of BTK function triggers an intrinsic B cell defect in BTK deficient mice²⁸, our findings that the response is intact in B cell deficient $Jh^{-/-}$ mice suggests B cell independent requirements for BTK in the MP-induced type 2 innate immune response.

IL-33 producing macrophages drive the type 2 MP response

The early BTK-dependent induction of IL-33 raised the possibility that this cytokine alarmin may promote the MP-induced type 2 immune response. Although not previously linked to sterile type 2 inflammation, IL-33 can drive type 2 responses in the context of helminth infection and allergic responses^{18, 31}. To determine the cellular sources of MP-induced IL-33 and associated type 2 cytokines, neutrophils (CD11b⁺, Ly6g⁺), eosinophils (Ly6g⁻, F4/80⁻, Siglec-F⁺), and macrophages (Ly6g⁻, Siglec-F⁻, F4/80⁺) were sort-purified from PECs for gene expression analysis at 2 days post MP inoculation. Macrophages were the major source of IL-33, while type 2 cytokines were differentially expressed by myeloid cells with neutrophils expressing elevated levels of IL-1 β and IL-13 and eosinophils expressing higher levels of IL-4 and IL-5 (Figure 2 A,B). Non-myeloid cells, which included any innate lymphoid cells, did not express significant levels of type 2 cytokines.

IL-33 may exert its biological effects by binding to its cell surface receptor, ST2, or as a nuclear transcription factor regulating the transcription of diverse inflammatory genes^{18, 32}. To examine the role of IL-33 in driving the MP-induced type 2 response, we blocked IL-33 function by directly neutralizing IL-33 with a recombinant soluble Fc-ST2 chimeric molecule 5 hours prior to and 24 hours after MP inoculation³³. As shown in Figure 2 (C–E), neutralization of IL-33 signaling blocked the inflammatory response 48 hours following MP inoculation. To confirm these results using a genetic approach, wild type (WT) or IL-33 receptor deficient (ST2^{-/-}) mice were inoculated intra-peritoneally with MPs and 2 days later PECs were collected and analyzed using flow cytometry and qPCR. ST-2 deficiency blocked MP mediated type 2 inflammation (Supplementary Figure 7 A,B). To assess whether the type 2 response can be rescued by exogenous IL-33 administration when BTK signaling is inhibited, we administered recombinant IL-33 (1 μ g/day) to Ibrutinib treated MP-inoculated mice and assessed inflammation at 48 hours. As shown in Figure 3A–C, IL-33 restored the innate type 2 responses. This rescue experiment thus indicates that BTK signaling is not required downstream of IL-33, consistent with a model where BTK triggers IL-33 which then initiates the type 2 innate response.

To investigate whether BTK signaling was also necessary for the helminth-induced type 2 immune response, BTK deficient and control mice wildtype mice were orally inoculated with 200 L3 of the murine intestinal nematode parasite, *Heligmosomoides polygyrus*. Elevations in myeloid cells, type 2 cytokines, and IL-4 bioactivity, as measured by mesenteric lymph node B cell MHCII elevations²⁹, were not impaired (Supplementary Figure 8). Our findings thus indicate that this robust type 2 response to multicellular parasites utilizes other BTK-independent pathways for initiation of the response. This alternative pathway triggered during helminth infection may involve epithelial cells and also ILC2 cells. Indeed, recent studies indicate that IL-33, TSLP, and IL-25 are redundant in some type 2 response models, including the immune response to *S. mansoni*, necessitating blockade of all three alarmins to inhibit the type 2 response³⁰. Apparently, initiation of MP-induced inflammation is instead dependent on BTK and associated IL-33 induction, raising the possibility that blockade of BTK or IL-33 may preferentially inhibit the response to MPs, leaving other immune responses, including those elicited by infectious agents, intact.

Adoptive transfer restores type 2 inflammation

Our findings indicated that after MP inoculation, IL-33 elevations and downstream type 2 immune responses were BTK-dependent and that the major source of IL-33 was macrophages. To assess whether BTK signaling in macrophages could restore IL-33 elevations and associated type 2 immunity in BTK deficient mice, 1×10^6 sort purified peritoneal macrophages, either from BTK deficient or WT mice, were adoptively transferred into recipient BTK deficient mice 24 hours prior to MP inoculation. Analysis of the inflammatory response 48 hours after MP inoculation showed significant increases in the immune cell infiltrate and cytokine responses in recipient BTK deficient mice with transferred WT macrophages. In parallel experiments transfer of macrophages from BTK deficient mice into recipient BTK deficient mice had little effect on the inflammatory response after MP inoculation (Fig 4 A–C). Thus, BTK signaling and associated IL-33 production in macrophages, are sufficient to drive the development of sterile inflammation in response to MP inoculation. Epithelial cells are generally thought to be critical in triggering type 2 immunity through their release of IL-33 and other alarmins^{31, 34}. Our studies now reveal that BTK signaling in macrophages induces their production of IL-33 and consequent initiation of the type 2 immune response. Previous studies have shown that activated macrophages can produce IL-33^{35, 36, 37}, although the significance of this observation in terms of immune response initiation has remained uncertain.

MPs directly promote IL-33 production by macrophages

To examine whether MPs could directly drive macrophage production of IL-33, highly purified peritoneal macrophages from untreated mice were cultured in vitro with MP and PF from MP-inoculated mice. As shown in Supplementary Figure 9, although MPs or PF alone had modest effects, the combination promoted marked increases in IL-33. To examine whether MP interactions with the macrophage, including phagocytosis, were involved, Cytochalasin D, which inhibits the assembly of actin filaments and phagocytosis^{38, 39}, was added to the cultures. Interestingly, cell death was significantly increased following culture of macrophages with MPs, which was blocked by Cytochalasin D. Physical interactions of the macrophage with the particle and IL-33 production were also markedly reduced. To assess whether cell death generally was important in triggering IL-33 production, inhibitors of necrosis (Necro2)^{40, 41}, and apoptosis (ZVED-FMK)⁴², were added. These inhibitors blocked MP-induced increases in IL-33. Taken together, these results indicate that phagocytic and other physical interactions of macrophages with MPs trigger cell death pathways that promote IL-33 production.

MP-induced inflammation in articular tissues

Although the peritoneal model provides a readily studied approach to investigate inflammatory responses to MPs, the response in joint tissue may be different and more clinically relevant. To investigate MP-induced inflammation in localized joint tissue we developed an experimental model, based on previous studies^{43, 44, 45}, where MPs are injected directly into the knee intra-articular region with 10mg of MPs in a 20ul volume. To examine the role of the SYK pathway, Bay 61–3606 was administered by oral gavage twice per day starting 2 days prior to bilateral intra-articular (i.a.) MP inoculation in the knee. As

seen from H&E stained slides and FACs analysis, 2 days after MP administration a robust inflammatory infiltrate was observed, which was inhibited by Bay 61–3606 (Figure 5A). We also examined effects of BTK signaling. Inhibition of BTK with Ibrutinib markedly reduced synovial inflammation (Figure 5B). To investigate whether MP induced joint inflammation was also dependent on IL-33, we administered intra-articular injections of either FcST2 or control IgG at day 0 and 1 after MP inoculation. Treatment with Fc-ST2 significantly reduced MP-induced joint inflammation (Figure 5C). Difficulty with isolation of viable immune cells from the murine joint tissue prevented reliable assessment of cytokine gene expression. Taken together, these data show that MP inoculation induces an inflammatory response in synovial tissues, similar to that seen in our peritoneal model and also dependent on SYK, BTK, and IL33 signaling. Recent studies indicate that different tissue microenvironments, which include tissue-resident macrophages and other immune and non-immune cells not present in peripheral blood, can support distinct responses^{46, 47}.

Apparently, immune stimulation in these different *in vivo* tissue milieus were sufficiently similar to support the development of a common innate response.

MPs promotes chronic inflammation and tissue damage

To more closely model the clinical case of articular tissues being repeatedly exposed to wear debris, we developed a repeated injection model of MP induced inflammation. In this model, bilateral intra-articular knee injections of MPs were given to C57BL/6 mice once per week over the course of 14 days. With this model, we examined both MP induced inflammation and potential pathology in peri-articular tissues. As shown in Supplementary Figure 10, repeated MP inoculations result in robust inflammation, including persistent presence of neutrophils and M2 macrophages and associated fibrosis. In addition the sustained chronic inflammation and fibrosis was associated with loss of both cartilaginous and osseous tissues. Taken together, these data suggest that a localized chronic type 2 innate immune response occurs in tissues repeatedly exposed to “wear debris” MPs.

Failed human joint arthroplasty reveals type 2 inflammation

Immunohistology was performed on periprosthetic and peri-articular tissue samples from patients undergoing revision total joint replacement or primary total joint arthroplasty. Multiple criteria were used to exclude any patients with septic tissues. H&E staining (Figure 6A–B) showed monocytic immune cell infiltration surrounding wear debris in periprosthetic tissue. Dual immunofluorescent staining for CD68 (macrophages) and either CD206 [mannose receptor (MRC1)] (Fig. 6C–D) or CD163 (Figure 6E–F) (both M2 markers) or iNOS (Figure 6G–H) (M1 marker) revealed increases in M2 macrophages in tissues from revision arthroplasty with increases in M1 macrophages predominantly in patients undergoing primary joint replacement.

Inflammatory response markers were assessed by qPCR. As shown in Figure 6I, M2 macrophage markers including Insulin-like growth factor 1 (IGF-1), Fibronectin 2 (FN2), Arg1, CCL18, MRC1 and chitinase-1 (CHIT1) were increased in patients undergoing revision surgery. Elevations in the type 2 cytokine, IL-13, and IL-33 were also detected in this group. These factors are characteristically activated in type 2 responses and human M2 macrophages⁴⁸. In contrast, IL-12, CXCR4, or iNOS expression, characteristic of M1

macrophages, were not elevated. Rigorous exclusion of patients with associated infections thus revealed the underlying type 2 inflammation triggered by implants.

In summary, our findings show that MPs induce cell death pathways in macrophages, which then express IL-33, thereby acting as essential players in the initiation of the type 2 sterile inflammatory response (see Supplementary Figure 11). Blockade of conventional signaling pathways associated with the type 1 inflammatory response, including Caspase-1 signaling, may have little effect on these responses. Instead our findings indicate that BTK signaling in macrophage initiates the sterile inflammatory response through its upregulation of the cytokine alarmin IL-33. Furthermore, these results suggest that BTK and IL-33 are potential therapeutic targets for controlling inflammatory responses triggered by MPs, including wear debris particles contributing to failure of fixation in orthopaedic implants.

Materials and Methods:

Mice

BALB/c, C57BL/6J, CBA/CaHN-*Btk*^{xid/J} and CBA/CaJ mice were obtained from the Jackson Laboratory (Bar Harbor, ME USA). Breeding pairs of DO11.10 TCR Transgenic BALB/c mice were obtained from The Jackson Laboratory and housed in a specific pathogen free facility during the experiments at Rutgers NJMS research animal facility, Newark, NJ. Caspase-1 KO mice were obtained from Dr. Thirumala-Devi Kanneganti (St Jude Hospital, Memphis, TN, USA) and B cell deficient *Jh*^{-/-} mice on BALB/c background were obtained from TACONIC Laboratory (Hudson, NY, USA). All mice for our experiments at Rutgers NJMS research animal facility were housed in a specific pathogen free, barrier facility excluding common adventitious pathogens. The studies have been reviewed and approved by the Institutional Animal Care and Use Committee at Rutgers—the State University of New Jersey. Experiments with *ST2*^{-/-} mice were performed at the Children's Hospital of Philadelphia, USA with the approval of The Children's Hospital of Philadelphia Institutional Animal Care and Use Committee. The experiments herein were conducted according to the principles set forth in the Guide for the Care and Use of Laboratory Animals, Institute of Animal Resources, National Research Council, Department of Health, Education and Welfare (US National Institutes of Health).

Dose and administration of microparticle (MP), inhibitors and blocking antibody.

Cobalt chrome microparticles (MPs) were obtained from Sandvik Osprey Ltd (Neath, Wales, UK). Sterile particles were prepared and redissolved in sterile PBS, as previously described¹⁰. These particles were separated using graded ethanol solution for sedimentation and analyzed by low-angle laser light scattering with a Microtrac X-100 (Bioengineering Solutions, Chicago, IL, USA). MPs ranging from 0.3 to 100µm were used and a dose of 50mg/mice was given intra-peritoneally for *in vivo* studies in mice. Bay 61-3606 was obtained from Sigma- Aldrich (St. Louis, MO, USA) and dissolved in Sterile PBS (vehicle) and C57BL/6 female mice (5-6 wks. old) were administered by oral gavage twice a day at a 10mg/kg body weight per day starting two days prior to inoculation of MPs. Ibrutinib was commercially obtained from Selleck Chemicals (Houston, TX, USA) and was dissolved in a vehicle consisting of 30% polyethylene glycol + 1% Tween80 +1% DMSO and filtered

through a 0.22 pore size filter (Durapore) obtained from Millipore (Billerica, MA, USA). A dose of 10mg/kg body weight of Ibrutinib was delivered by oral gavage with a gavage-feeding needle once a day starting one day prior to microparticles inoculation. Recombinant IL33/Vehicle (1µg/day) (R&D system, Minneapolis, MN, USA) was administered (i.p.) to Ibrutinib treated mice. To abrogate in vivo CD4⁺ T cell function, 1mg of anti-CD4 mAb (GK1.5) (BioXcell, West Lebanon, NH, USA) was given i.p. one day before microparticles inoculation. CD4⁺ T cell depletion was confirmed by flow cytometry of lymph node cell suspensions. In order to block the IL-33 signaling pathways, we administered MP inoculated mice with 7.5 µg of either recombinant human IgG1Fc (isotype Fc) or recombinant mouse ST2/IL-33RfC (R&D system, Minneapolis, MN, USA) intraperitoneally, 5 hours prior to MP inoculation and again another dose on day 1 after MP inoculation. IL33 signaling in the knee synovium was blocked by combined intra-articular (5µg) and peritoneal (2.5µg) administration of either Fc-ST2 or control IgG at day 0 and day 1 after MP inoculation.

Flow cytometry

Peritoneal exudate cell (PEC) suspensions were blocked with Fc Block (BD Biosciences, San Jose, CA, USA) and subsequently stained with specific Abs including: anti-Ly6G FITC, anti-CD11cPE, anti-CD11b PerCP/Cy5.5, Siglec-F PE, anti-c-kit APC, F4/80 APC, anti-CD4APC, anti-CD19 PerCP/Cy5.5, CD3PE (BD Biosciences, San Jose, CA, USA) and anti-CD206PE or anti-CD206 Alexa fluor 488 (Biolegend, USA). Cells were collected 4 hours after microparticle inoculation for analysis of phosphorylation of BTK (Y-551) or SYK (Y-348). Intracellular staining was performed using anti-mouse phospho-BTK/ITK (Y551/Y511) PE (eBiosciences, San Diego, CA, USA), anti-mouse phospho-SYK (Y-348) PE antibody (BD Biosciences, San Jose, CA, USA) and FOXP3/Transcription Factor Staining Buffer Set, which was used as per the manufacturer instructions (eBiosciences, San Diego, CA, USA). For CFSE-labeled cells, anti-CD4 PerCP (BD Biosciences, San Jose, CA, USA), and KJ1-26 PE (BD Biosciences, San Jose, CA, USA) were used to phenotype DO11.10 T cells and cell cycle progression was examined as previously discussed¹⁰. For FACS analysis of whole synovial tissues, samples were digested at 37°C for 1 hour with 0.1% collagenase in RPMI supplemented with 10% FBS, 1000U/ml penicillin, 1000U/ml streptomycin, and 2mM L-glutamine. Single cell suspensions were then prepared and blocked and stained as described above.

Sorting and adoptive transfer of peritoneal innate cell populations

For gene expression analysis of peritoneal innate cell populations, peritoneal exudate cells were harvested from C57BL/6 wild type mice and were separated through electronic sorting employing FACS Aria II (BD Biosciences, San Jose, USA) (see Supplementary Figure 12 for gating strategy). For adoptive transfer experiments, macrophages were purified from wild type (CBA/J) or BTK mutant Mice (CBA/N^{XID}) with biotin anti-mouse F4/80 antibody (Biolegend, USA) and anti-biotin bead obtained from Miltenyi Biotec, USA. Twenty-four hours before MP inoculation, 1×10⁶ peritoneal macrophages from either XID or wild type (WT) mice were transferred to XID recipient mice.

***In vitro* microparticle (MP) culture with sorted macrophages**

Peritoneal exudate cells (PECs) were collected from C57BL/6 wild type mice and macrophages were separated (>95% pure) using biotinylated anti-mouse F4/80 antibody (Biolegend, USA) followed by anti-biotin beads (Miltenyi Biotec, USA). 0.25 million purified macrophages were cultured with 0.25mg MPs in media containing 2% peritoneal fluid (PF) harvested from MP inoculated mice. In some cultures, inhibitors of necrosis [30 μ M Necrox2 (Enzo Life Sciences, INC., USA)] apoptosis [100 μ M ZVED-FMK (R&D Systems, Inc., USA)], and phagocytosis [(2 μ M) Cytochalasin-D (Enzo Life Sciences, INC., USA)] were added. After 48 hrs, supernatants were assayed for IL33 as already described above (IL-33 bioassay). The % of necrosis was determined by staining cells with acridine orange and propidium iodide (AOPIstain, Nexcelom Bioscience, USA) and cells were assayed for viability by using Cellometer Auto2000 (Nexcelom Bioscience, USA). To assess MP/macrophage interactions following Cytochalasin-D administration, the percent of macrophages with associated MPs were determined using images (40 \times) obtained with the EVOS XL Core microscope (Life Technology, USA).

Adoptive transfers of D011.10 TCR CD4⁺ T cells

Spleen and lymph nodes were collected from WT DO11.10 TCR-transgenic mice. DO11.10 OVA-specific TCR transgenic CD4⁺ cells were isolated, CFSE-labeled, and adoptively transferred to recipient BALB/c mice intravenously, as previously described¹⁰. Thirty μ g OVA peptide alone or with either 50mg microparticles or with 4 mg alum were injected i.p. into the recipient mice 2 days after transfer. HPLC-purified OVA₃₂₃₋₃₃₉ (OVA peptide) was synthesized at the Rutgers-NJMS Molecular Resources Facility (MRF) core facility.

Intra-articular immunization with microparticles (MPs)

Mice were given bilateral intra-articular knee injections with either vehicle or 10mg of microparticle in a 20ul volume. Knee tissues were collected after 2 days, fixed in 10% buffered formalin, and decalcified by EDTA. The slides were examined using a Zeiss Axioscope2 and the images were captured and analyzed by Axiovision (Thornwood, NY, USA) software in 100 \times magnification. The area of immune cell infiltration and the total synovial tissue area were measured using Axiovision software. We also developed a repeated injection model of MP induced chronic inflammation. In this model, intra-articular MP inoculations of the knee were given once per week over the course of 14 days. For pathologic analysis, formalin fixed tissue samples were decalcified with EDTA, sections were picosirius red stained and digitally imaged to assess the level of fibrosis. For cartilage analysis, sections were Safranin-O stained. For analysis of changes to osseous tissue and inflammation H and E stained slides were used.

Parasite Inoculation and characterization of cells

Two hundred infective Hp L3 were inoculated in mice using a rounded gavage tube, and at day 7, peritoneal cells and mesenteric lymph nodes were harvested. Flow cytometric analysis of PEC was performed as described above for MPs. For B cells, expression of MHCII was monitored by flow cytometer using B220, CD3 and MHCII from BD

Biosciences, and used as per manufacturer's instructions. MLNs were also analyzed for gene expression as described above.

Immunofluorescence Microscopy

Human tissue samples from primary and revision arthroplasty were fresh frozen and sectioned at 5 μ m with an HM505E cryostat. Samples were fixed in acetone at -20°C and blocked using Protein Block (Dako, Carpinteria, CA, USA), FcX (Biolegend, San Jose, CA, USA) and 10% normal goat serum (Jackson ImmunoResearch, West Grove, PA, USA). The primary antibodies used were mouse anti-human CD68, biotin anti-CD206, biotin anti-CD163 (Biolegend, San Jose, CA, USA), and rabbit anti-human iNOS (Abcam, Cambridge, MA, USA). The secondary antibodies used were AF488-conjugated goat anti-mouse, AF555-conjugated goat anti-rabbit and Streptavidin Rhodamine Red-X (Invitrogen, Eugene, Oregon, USA). Nuclear staining was performed using Vectashield with DAPI (Vector Laboratories, Burlingame, CA, USA). Digital images were obtained with a Leica DM6000B and a Hamamatsu Orca-Flash 4.0 camera and tiled using Leica Application Suites Advanced Fluorescence (Leica Microsystems, Buffalo Grove, IL, USA). Fluorescence intensities and exposure times were normalized to appropriate control images.

ELISPOT

Single-cell lymph node suspensions were cultured with 10 $\mu\text{g}/\text{ml}$ OVA peptide for 3 days on anti-IL-4 (Clone BVD4-1D11.2, BD Biosciences, San Jose, CA, USA) or anti-IFN- γ (BD Biosciences, San Jose, CA, USA) coated plates and after 72 hours plates were washed, incubated overnight with secondary biotinylated anti-IL-4 or anti-IFN- γ Abs, and then developed with Streptavidin-alkaline phosphatase (Jackson Immuno Research Laboratories, West Grove, PA, USA) as previously described¹⁰. Results were quantitated by counting the number of positive colonies under a microscope.

Bioassays of IL-1 β and IL33 in peritoneal fluid

Four hours after MP inoculation, the peritoneum was flushed with 1ml of sterile PBS and the cell suspension was centrifuged and the supernatant was collected and then stored at -80°C . ELISA was performed using either IL1- β or IL33 Ready-Set-Go! (eBioscience, San Diego, CA, USA) as per the manufacturer's instructions.

CD4⁺ and DO11.10 T cell sorting

Single cell suspensions from lymph nodes of DO11.10 mice were incubated with anti-CD4 micro beads (Miltenyi Biotec, San Diego, CA, USA) and CD4⁺ T cells were sort purified. The KJ1-26⁺ population was then positively selected as previously described¹⁰. Sorted populations were 85-90% pure.

Quantitation of cytokine gene expression

Total RNA was extracted from PECs with Trizol (Invitrogen, Eugene, Oregon, USA). RNA extraction from human and murine synovial tissues was performed using RNA-Bee (Amsbio, Milton, Abingdon, U.K.). Isolated RNA was reverse transcribed using Super Script II reverse transcriptase (Invitrogen, Eugene, Oregon, USA). The gene specific

Taqman assay (Applied Biosystems, Waltham, MA, USA) was used for amplification and detection of different genes with Applied Biosystems 7500 sequence detector. Gene expression fold changes of different mRNA of treated samples were quantified relative to the untreated after normalizing to 18s RNA, as previously described¹⁰.

Collection and analysis of clinical tissue samples

Prospective clinical studies were approved by an Institutional Review Board (IRB) protocol. Periprosthetic and peri-articular tissue samples were collected from human subjects undergoing revision total joint replacements or primary total joint arthroplasty respectively. Primary joint arthroplasty samples served as controls for all experiments. Multiple criteria were used to exclude septic loosening, using previously described methods⁴⁹, including analysis of erythrocyte sedimentation rates, C-reactive protein (CRP) levels, and culturing of tissue and joint aspirates. Retrieved tissues were frozen for subsequent cryo-sectioning or homogenized for RNA purification.

Statistical analysis

The mean \pm standard error of the mean (SE) is indicated in relevant figures. Statistical analyses included ANOVA followed by individual two-way comparisons with Tukey test or paired T test using Graphpad Prism version 6.0 (Graph Pad Software Inc., La Jolla, CA, USA). Statistical differences at a level of $p < 0.05$ between groups was considered significant.

Institutional Review Board (IRB) Study Approval

Proposed human studies for this investigation were approved by the Rutgers - New Jersey Medical School IRB. All investigations were conducted in conformity with ethical principles of research, and informed consent for participation in the study was obtained. All investigations involving human subjects were performed at Rutgers, New Jersey Medical School, Newark, NJ.

Supplementary Material

Refer to Web version on PubMed Central for supplementary material.

Acknowledgements

This grant was supported by National Institutes of Health grants: R01DK11379002, R01AI13163401A1, R01AI121250, R01AI101935, RO1AI124346, RO1AR060782, and R01AI114647-01A1. We would like to acknowledge Sandvik Osprey Powders, UK for generously providing the micron sized CoCr material used in this paper. In addition we would like to thank Dr. Edward M. Adler, Dr. Mark C. Riley, Dr. Francis R. Patterson, and Dr. John S. Hwang (Dept. of Orthopaedic Surgery, NJMS, Rutgers) and Dr. Stephen R. Peters (Department of Pathology and Laboratory Medicine) for providing clinical samples and assistance in tissue preparation.

References:

1. Kurtz S, Ong K, Lau E, Mowat F & Halpern M Projections of primary and revision hip and knee arthroplasty in the United States from 2005 to 2030. *J Bone Joint Surg Am* 89, 780–785 (2007). [PubMed: 17403800]
2. Cobelli N, Scharf B, Crisi GM, Hardin J & Santambrogio L Mediators of the inflammatory response to joint replacement devices. *Nat Rev Rheumatol* 7, 600–608 (2011). [PubMed: 21894210]

3. Goodman SB et al. Novel biological strategies for treatment of wear particle-induced periprosthetic osteolysis of orthopaedic implants for joint replacement. *Journal of the Royal Society, Interface /the Royal Society* 11, 20130962 (2014).
4. Veisoh O et al. Size- and shape-dependent foreign body immune response to materials implanted in rodents and non-human primates. *Nat Mater* 14, 643–651 (2015). [PubMed: 25985456]
5. Antonios JK, Yao Z, Li C, Rao AJ & Goodman SB Macrophage polarization in response to wear particles in vitro. *Cellular & molecular immunology* 10, 471–482 (2013). [PubMed: 24013843]
6. Nakashima Y et al. Signaling pathways for tumor necrosis factor-alpha and interleukin-6 expression in human macrophages exposed to titanium-alloy particulate debris in vitro. *J Bone Joint Surg Am* 81, 603–615 (1999). [PubMed: 10360689]
7. Potnis PA, Dutta DK & Wood SC Toll-like receptor 4 signaling pathway mediates proinflammatory immune response to cobalt-alloy particles. *Cell Immunol* 282, 53–65 (2013). [PubMed: 23680697]
8. Bi Y, Collier TO, Goldberg VM, Anderson JM & Greenfield EM Adherent endotoxin mediates biological responses of titanium particles without stimulating their phagocytosis. *J Orthop Res* 20, 696–703 (2002). [PubMed: 12168657]
9. Greenfield EM, Beidelschies MA, Tatro JM, Goldberg VM & Hise AG Bacterial pathogen-associated molecular patterns stimulate biological activity of orthopaedic wear particles by activating cognate Toll-like receptors. *J Biol Chem* 285, 32378–32384 (2010). [PubMed: 20729214]
10. Mishra PK et al. Micrometer-sized titanium particles can induce potent Th2-type responses through TLR4-independent pathways. *J Immunol* 187, 6491–6498 (2011). [PubMed: 22095717]
11. Kool M et al. An unexpected role for uric acid as an inducer of T helper 2 cell immunity to inhaled antigens and inflammatory mediator of allergic asthma. *Immunity* 34, 527–540 (2011). [PubMed: 21474346]
12. Kuroda E et al. Silica crystals and aluminum salts regulate the production of prostaglandin in macrophages via NALP3 inflammasome-independent mechanisms. *Immunity* 34, 514–526 (2011). [PubMed: 21497116]
13. Rathinam VA, Vanaja SK & Fitzgerald KA Regulation of inflammasome signaling. *Nat Immunol* 13, 333–342 (2012). [PubMed: 22430786]
14. Mayer-Barber KD et al. Caspase-1 independent IL-1beta production is critical for host resistance to mycobacterium tuberculosis and does not require TLR signaling in vivo. *Journal of immunology* 184, 3326–3330 (2010).
15. Ng G et al. Receptor-independent, direct membrane binding leads to cell-surface lipid sorting and Syk kinase activation in dendritic cells. *Immunity* 29, 807–818 (2008). [PubMed: 18993083]
16. Flach TL et al. Alum interaction with dendritic cell membrane lipids is essential for its adjuvanticity. *Nat Med* 17, 479–487 (2011). [PubMed: 21399646]
17. Yamamoto N et al. The orally available spleen tyrosine kinase inhibitor 2-[7-(3,4-dimethoxyphenyl)-imidazo[1,2-c]pyrimidin-5-ylamino]nicotinamide dihydrochloride (BAY 61–3606) blocks antigen-induced airway inflammation in rodents. *J Pharmacol Exp Ther* 306, 1174–1181 (2003). [PubMed: 12766258]
18. Schmitz J et al. IL-33, an interleukin-1-like cytokine that signals via the IL-1 receptor-related protein ST2 and induces T helper type 2-associated cytokines. *Immunity* 23, 479–490 (2005). [PubMed: 16286016]
19. Whang JA & Chang BY Bruton’s tyrosine kinase inhibitors for the treatment of rheumatoid arthritis. *Drug discovery today* 19, 1200–1204 (2014). [PubMed: 24721226]
20. Baba Y et al. BLNK mediates Syk-dependent Btk activation. *Proc Natl Acad Sci U S A* 98, 2582–2586 (2001). [PubMed: 11226282]
21. Shinohara M et al. The orally available Btk inhibitor ibrutinib (PCI-32765) protects against osteoclast-mediated bone loss. *Bone* 60, 8–15 (2014). [PubMed: 24316417]
22. Pan Z et al. Discovery of selective irreversible inhibitors for Bruton’s tyrosine kinase. *ChemMedChem* 2, 58–61 (2007). [PubMed: 17154430]
23. Honigberg LA et al. The Bruton tyrosine kinase inhibitor PCI-32765 blocks B-cell activation and is efficacious in models of autoimmune disease and B-cell malignancy. *Proc Natl Acad Sci U S A* 107, 13075–13080 (2010). [PubMed: 20615965]

24. Dubovsky JA et al. Ibrutinib is an irreversible molecular inhibitor of ITK driving a Th1-selective pressure in T lymphocytes. *Blood* 122, 2539–2549 (2013). [PubMed: 23886836]
25. Anthony RM et al. Memory T(H)2 cells induce alternatively activated macrophages to mediate protection against nematode parasites. *Nat Med* 12, 955–960 (2006). [PubMed: 16892038]
26. Thomas JD et al. Colocalization of X-linked agammaglobulinemia and X-linked immunodeficiency genes. *Science* 261, 355–358 (1993). [PubMed: 8332900]
27. Rawlings DJ et al. Mutation of unique region of Bruton’s tyrosine kinase in immunodeficient XID mice. *Science* 261, 358–361 (1993). [PubMed: 8332901]
28. Khan WN et al. Defective B cell development and function in Btk-deficient mice. *Immunity* 3, 283–299 (1995). [PubMed: 7552994]
29. Mishra PK, Patel N, Wu W, Bleich D & Gause WC Prevention of type 1 diabetes through infection with an intestinal nematode parasite requires IL-10 in the absence of a Th2-type response. *Mucosal Immunol* 6, 297–308 (2013). [PubMed: 22806101]
30. Vannella KM et al. Combinatorial targeting of TSLP, IL-25, and IL-33 in type 2 cytokine-driven inflammation and fibrosis. *Sci Transl Med* 8, 337ra365 (2016).
31. Sonnenberg GF & Artis D Innate lymphoid cells in the initiation, regulation and resolution of inflammation. *Nat Med* 21, 698–708 (2015). [PubMed: 26121198]
32. Carriere V et al. IL-33, the IL-1-like cytokine ligand for ST2 receptor, is a chromatin-associated nuclear factor in vivo. *Proc Natl Acad Sci U S A* 104, 282–287 (2007). [PubMed: 17185418]
33. Liu T et al. Aspirin-Exacerbated Respiratory Disease Involves a Cysteinyl Leukotriene-Driven IL-33-Mediated Mast Cell Activation Pathway. *J Immunol* 195, 3537–3545 (2015). [PubMed: 26342029]
34. Gause WC, Wynn TA & Allen JE Type 2 immunity and wound healing: evolutionary refinement of adaptive immunity by helminths. *Nat Rev Immunol* 13, 607–614 (2013). [PubMed: 23827958]
35. Qi F et al. Macrophages produce IL-33 by activating MAPK signaling pathway during RSV infection. *Molecular immunology* 87, 284–292 (2017). [PubMed: 28531812]
36. Fock V et al. Macrophage-derived IL-33 is a critical factor for placental growth. *J Immunol* 191, 3734–3743 (2013). [PubMed: 23997215]
37. Chang YJ et al. Innate lymphoid cells mediate influenza-induced airway hyper-reactivity independently of adaptive immunity. *Nat Immunol* 12, 631–638 (2011). [PubMed: 21623379]
38. Casella JF, Flanagan MD & Lin S Cytochalasin D inhibits actin polymerization and induces depolymerization of actin filaments formed during platelet shape change. *Nature* 293, 302–305 (1981). [PubMed: 7196996]
39. Kim SM et al. TREM2 promotes Abeta phagocytosis by upregulating C/EBPalpha-dependent CD36 expression in microglia. *Sci Rep* 7, 11118 (2017). [PubMed: 28894284]
40. Degtarev A et al. Chemical inhibitor of nonapoptotic cell death with therapeutic potential for ischemic brain injury. *Nat Chem Biol* 1, 112–119 (2005). [PubMed: 16408008]
41. Cui H et al. Necrostatin-1 treatment inhibits osteocyte necroptosis and trabecular deterioration in ovariectomized rats. *Sci Rep* 6, 33803 (2016). [PubMed: 27703177]
42. Gastman BR, Johnson DE, Whiteside TL & Rabinowich H Caspase-mediated degradation of T-cell receptor zeta-chain. *Cancer Res* 59, 1422–1427 (1999). [PubMed: 10197606]
43. Amaral FA et al. NLRP3 inflammasome-mediated neutrophil recruitment and hypernociception depend on leukotriene B(4) in a murine model of gout. *Arthritis and rheumatism* 64, 474–484 (2012). [PubMed: 21952942]
44. van Beuningen HM, Glansbeek HL, van der Kraan PM & van den Berg WB Osteoarthritis-like changes in the murine knee joint resulting from intra-articular transforming growth factor-beta injections. *Osteoarthritis and cartilage /OARS, Osteoarthritis Research Society* 8, 25–33 (2000).
45. Zhang T et al. The effect of osteoprotegerin gene modification on wear debris-induced osteolysis in a murine model of knee prosthesis failure. *Biomaterials* 30, 6102–6108 (2009). [PubMed: 19665222]
46. Hashimoto D et al. Tissue-resident macrophages self-maintain locally throughout adult life with minimal contribution from circulating monocytes. *Immunity* 38, 792–804 (2013). [PubMed: 23601688]

47. Jenkins SJ et al. IL-4 directly signals tissue-resident macrophages to proliferate beyond homeostatic levels controlled by CSF-1. *J Exp Med* 210, 2477–2491 (2013). [PubMed: 24101381]
48. Martinez FO, Gordon S, Locati M & Mantovani A Transcriptional profiling of the human monocyte-to-macrophage differentiation and polarization: new molecules and patterns of gene expression. *Journal of immunology* 177, 7303–7311 (2006).
49. Koulouvaris P et al. Expression profiling reveals alternative macrophage activation and impaired osteogenesis in periprosthetic osteolysis. *J Orthop Res* 26, 106–116 (2008). [PubMed: 17729302]

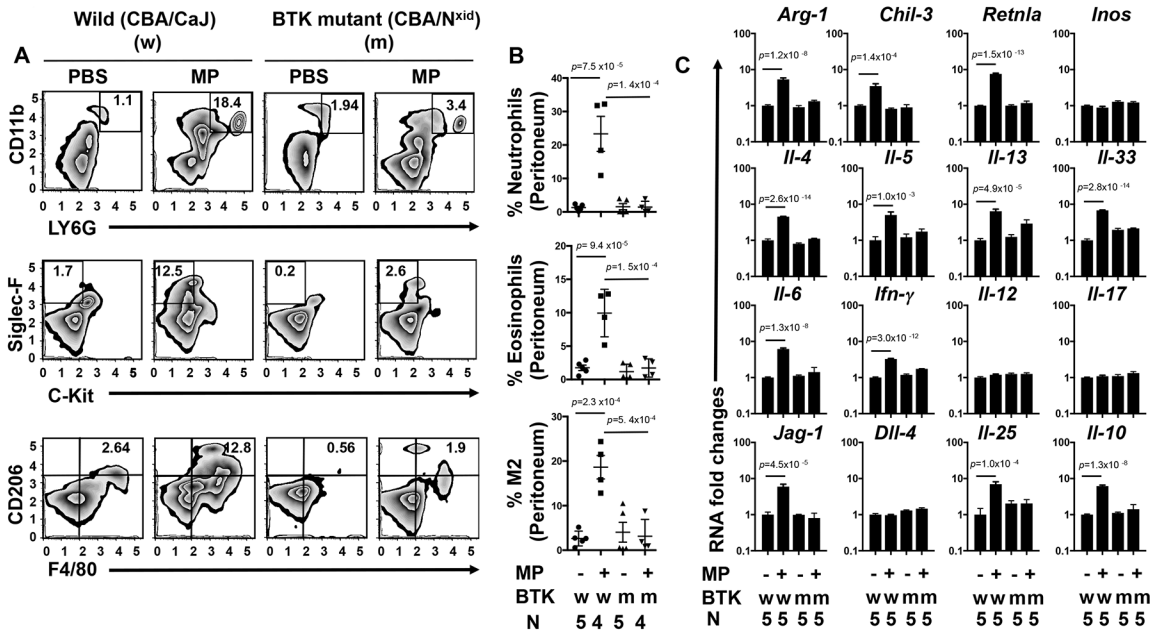


Figure 1: The microparticle (MP) induced type 2 innate response is dependent on BTK signaling
 Wild type (CBA/CaJ) (W) or BTK mutant (CBA/N^{XID}) (m) mice were inoculated i.p. with either PBS or microparticles (MPs). Forty-eight hours later peritoneal cells (PECs) were collected and stained for neutrophils (CD11b PerCP/Cy5.5⁺, Ly6G FITC⁺), eosinophils (c-Kit APC⁻, Siglec-F PE⁺), and alternatively activated (M2) macrophages (F4/80 APC⁺, CD206 Alexa Fluor 488⁺). FACS analyses are presented as representative plots (A) or graphically as the percentage of total peritoneal cells in each sample (B). RNA extracted from PECs was analyzed by qPCR for mRNA species characteristic of M2 macrophages (*Arg-1*, *Chi3l3*, *Retnla*) and cytokines representative of type 1, 2, and 17 responses (C). The mean and se is shown for each treatment group along with the exact p values and number (N) of individual mice, 4 or 5/treatment group, which varied with availability of mice. No outliers were removed from analyses and measurements were taken from distinct samples. Statistical analyses were performed by One way ANOVA followed by Tukey multiple comparisons using GrapPad-Prism software. All experiments were performed two times with similar results.

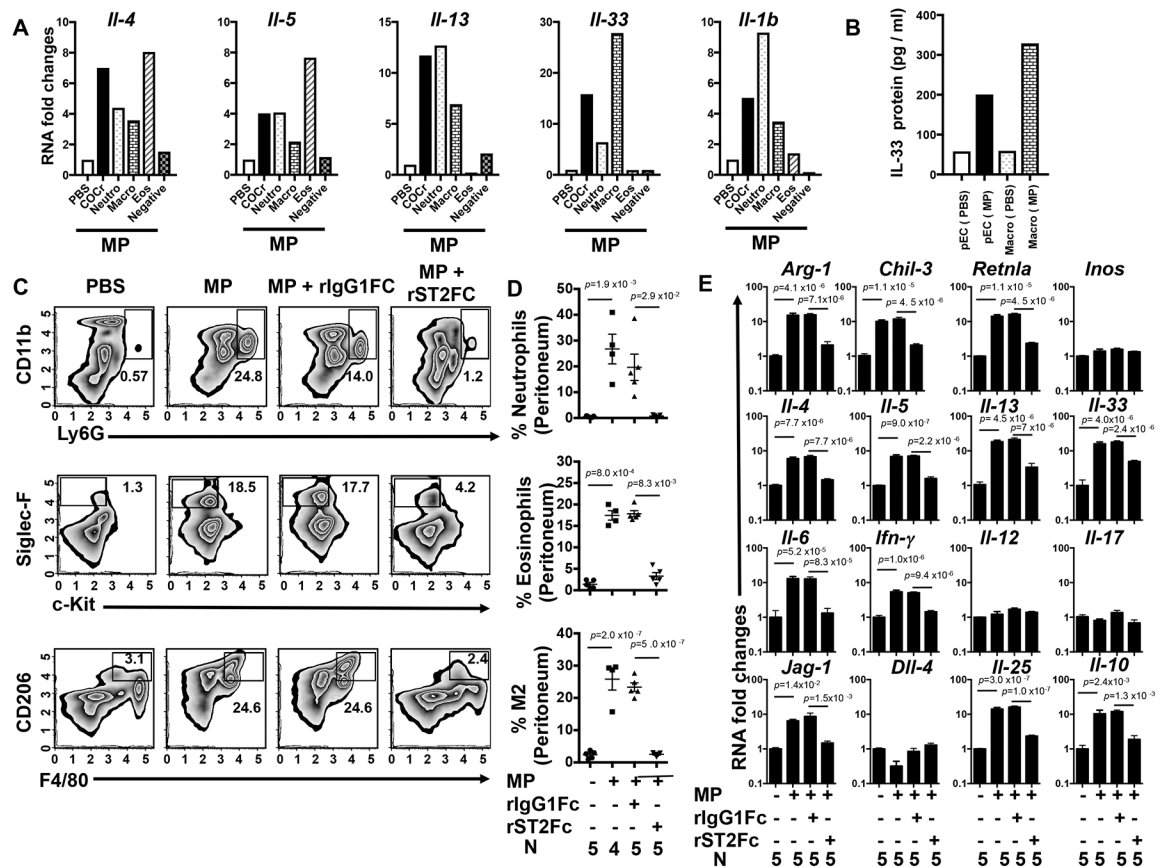


Fig 2: Macrophages are the primary source of IL-33 and IL-33 blockade inhibits the type 2 response

Five C57BL/6 mice were inoculated i.p. with vehicle or microparticles (MPs) and peritoneal cells (PECs) were collected after 48 hours. PECs were pooled from individual mice and neutrophils were electronically sorted as CD11b PerCP/Cy5.5⁺, Ly6G FITC⁺ cells. Non-neutrophil cells (CD11b PerCP/Cy5.5⁺, Ly6G FITC⁻) were sort purified for eosinophils (Siglec-F PE⁺, F4/80 APC⁻), macrophages (F4/80 APC⁺, Siglec-F PE⁻), and cells negative for above markers. RNA extracted from sorted cell populations was analyzed by qPCR for *Il-4*, *Il-5*, *Il-13*, *Il-33*, and *Il-1b* mRNA (A). Total PECs and sorted macrophages from PBS or MP treated mice (5/treatment group) were incubated overnight and supernatants assessed for IL-33 by ELISA (B). Experiments A and B were performed twice with similar results. In a separate experiment, C57BL/6 mice were inoculated i.p. with vehicle or MP and administered recombinant ST2/IL-33R Fc or control IgG1Fc. Forty-eight hours later PECs were collected and stained for flow cytometry with antibodies specific for neutrophils (CD11b PerCP/Cy5.5⁺, Ly6G FITC⁺), eosinophils (c-Kit APC⁻, Siglec-F PE⁺), and alternatively activated (M2) macrophages (F4/80 APC⁺, CD206 Alexa Fluor 488⁺) and plotted either as a representative plot (C) or as a graph showing the percentage of individual cells/total PECs (D). PEC RNA was analyzed by qPCR for markers characteristic of M2 macrophages and cytokines representative of type 1, type 2, and type 17 responses (E). For D-E, the mean and se are shown for each treatment group along with the exact P values and the number (N) of individual mice, 4 or 5/treatment group, which varied with availability of

mice. No outliers were removed from analyses and measurements were taken from distinct samples. Statistical tests are as described in Fig. 1. All experiments were performed two times with similar results.

Author Manuscript

Author Manuscript

Author Manuscript

Author Manuscript

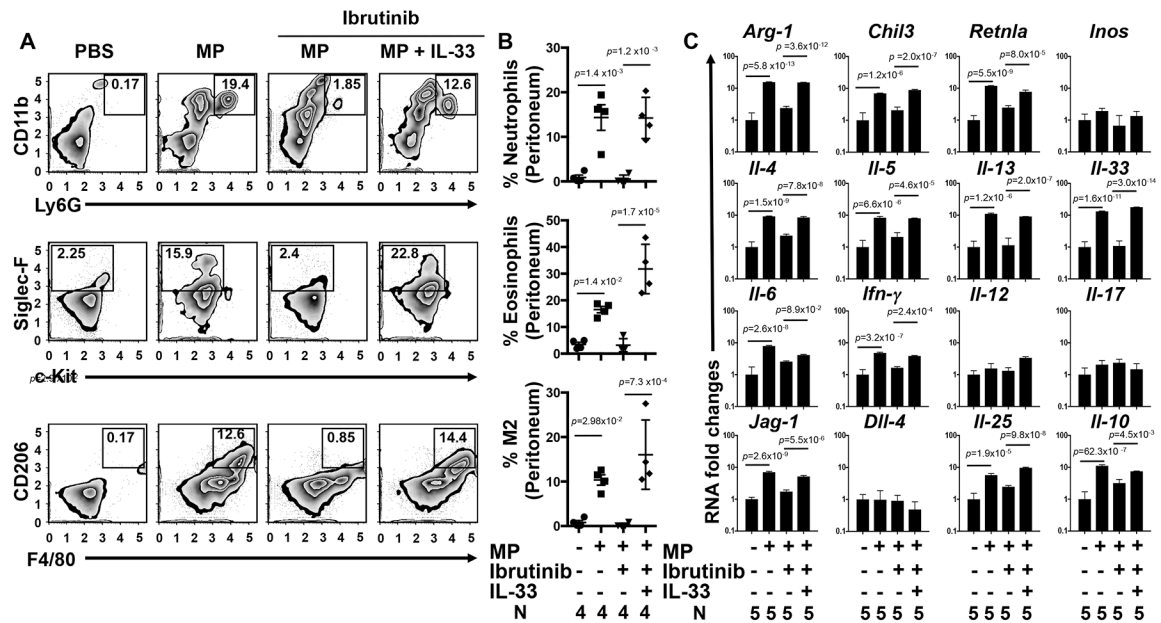


Fig 3: IL-33 restores the microparticle (MP) induced response following Bruton's tyrosine kinase (BTK) inhibition

C57BL/6 mice were inoculated i.p. with vehicle or MPs and treated with either vehicle or with the BTK inhibitor, ibrutinib. Recombinant IL-33 or vehicle (1 μ g/day) was administered (i.p.) to ibrutinib treated mice. Forty-eight hours after MP inoculation, peritoneal cells (PECs) were collected and then stained for flow cytometry with specific antibodies for detection of neutrophils (CD11b PerCP/Cy5.5⁺, Ly6G FITC⁺), eosinophils (c-Kit APC⁻, Siglec-F PE⁺), and alternatively activated (M2) macrophages (F4/80 APC⁺, CD206 Alexa Fluor 488⁺) and plotted as a representative plot (A) and as a graph showing the percentage of individual innate immune cells/total PEC population (B). RNA extracted from the PECs was analyzed by qPCR for mRNA species characteristic of M2 macrophages and other cytokines representative of the type 1, 2, and 17 responses (C). For B-C, the mean and se is shown for each treatment group along with the exact p values and the number (N) of individual mice, 4 or 5/treatment group, which varied with availability of mice. No outliers were removed from analyses and measurements were taken from distinct samples. Statistical tests are as described in Fig. 1. All experiments were performed two times with similar results.

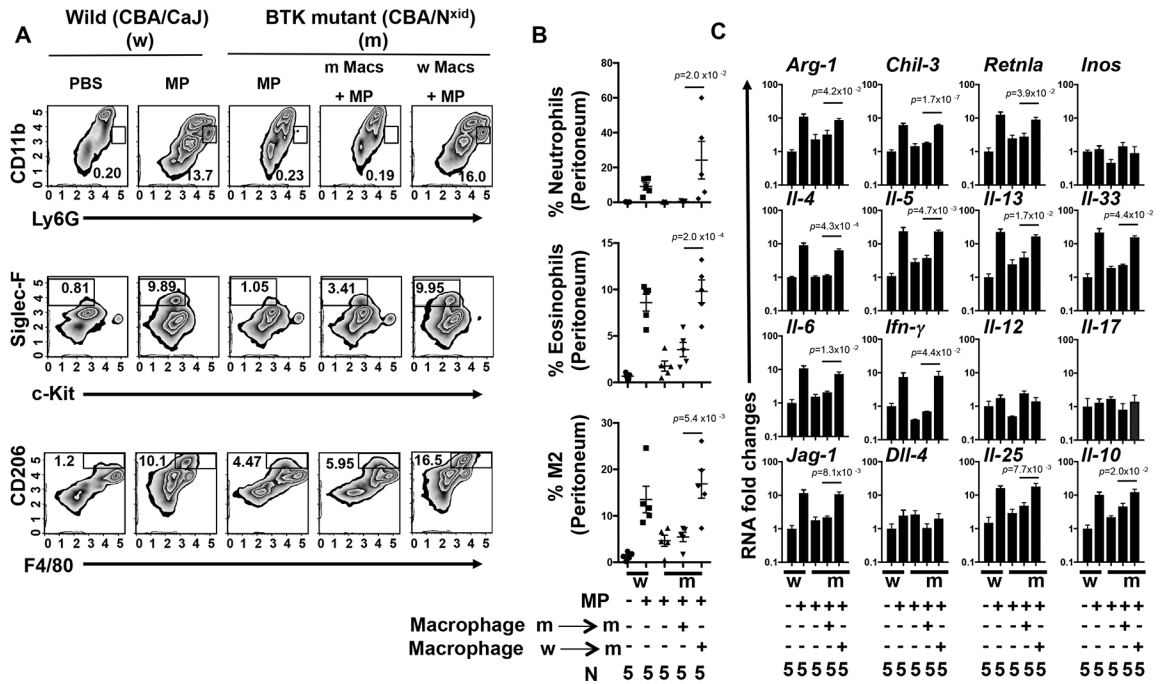


Fig 4: Macrophages rescue type 2 inflammation in BTK deficient (XID) mice
 Control wild type (CBA/CaJ) (W) or BTK mutant (CBA/N^{XID}) (m) mice were inoculated i.p. with vehicle 4 hours prior to macrophage isolation. 24 hours before MP inoculation, 1×10^6 peritoneal macrophages either from XID (m) or wild type (w) mice were transferred to XID (m) recipient mice. Forty-eight hours after MP inoculation, peritoneal cells were collected and then stained for flow cytometry with specific antibodies for neutrophils (CD11b PerCP/CY5.5⁺, Ly6G FITC⁺), eosinophils (c-Kit APC⁻, Siglec-F PE⁺), and alternatively activated (M2) macrophages (F4/80 APC⁺, CD206 Alexa Fluor 488⁺) and plotted either as a representative plot (A) or as a graph showing the percentage of individual innate immune cells/total peritoneal cell population (B). RNA extracted from the peritoneal cells was analyzed by qPCR for mRNA species characteristic of M2 macrophages and other cytokines representative of the Type 1, Type 2, and Type 17 responses (C). For B-C, the mean and se is shown for each treatment group along with the exact p values and the number (N) of individual mice, (5)/treatment group. No outliers were removed from analyses and measurements were taken from distinct samples. Statistical tests are as described in Fig. 1. All experiments were performed two times with similar results.

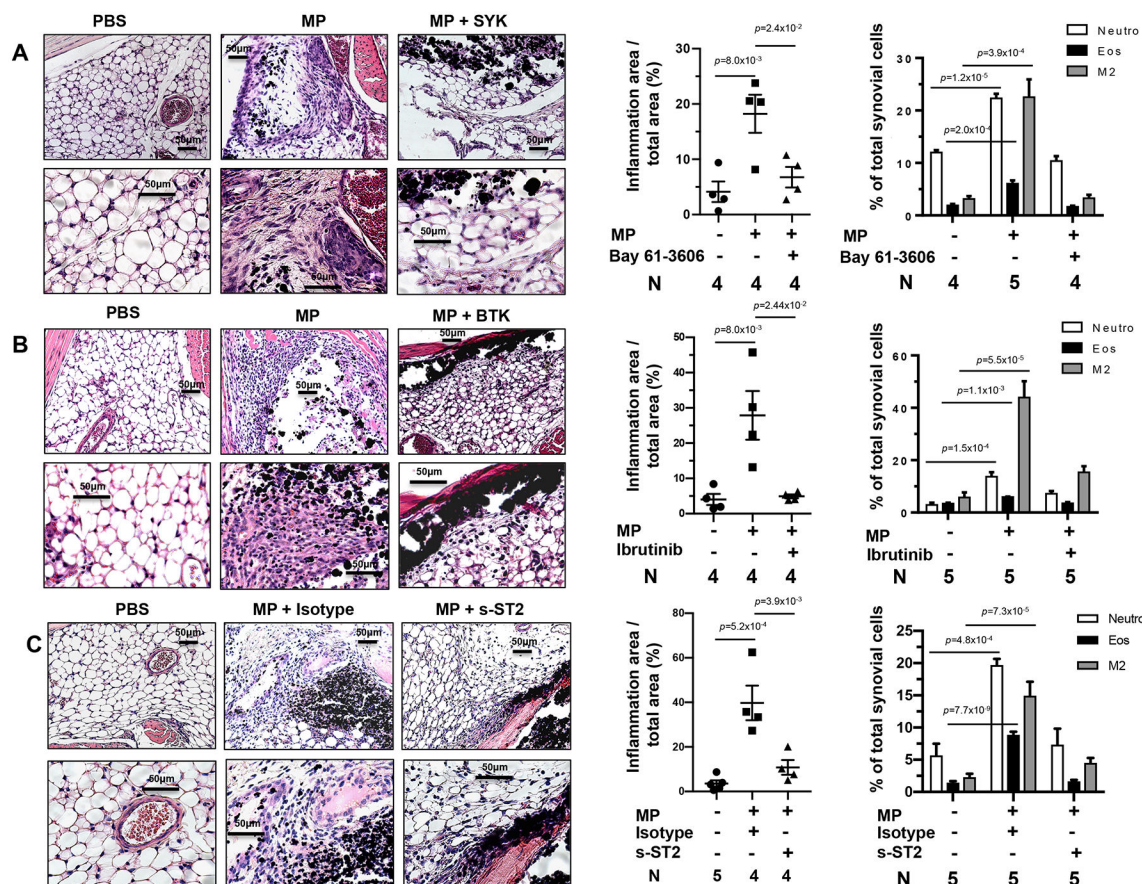


Fig 5: Microparticle (MP) induced articular tissue inflammation is SYK, BTK and IL33 dependent.

C57BL/6 mice were administered bilateral intra-articular knee injections with PBS vehicle or MPs. For SYK inhibition studies (A), either vehicle or Bay 61–3606 was administered 2 days prior to MP inoculation. For BTK inhibition studies (B), either vehicle or Ibrutinib was administered 1 day prior to MP inoculation. For blockade of IL33 signaling (C), the mice were administered either Isotype control Ab or recombinant sST2 by Intra-peritoneal and intra-articular knee injection. For all studies, whole hind limbs were collected 2 days after MP inoculation. For pathologic analysis, formalin fixed tissue samples were decalcified with EDTA, sections were H&E stained and digitally imaged. Scale bars (50µm) are shown for each image. The extent of inflammation was digitally quantitated as area of synovial inflammation/total area of synovium and graphed. For FACs analysis, samples were digested at 37°C for 1 hour with collagenase and single cell suspensions were stained for flow cytometry with specific antibodies for neutrophils (CD11b PerCP/CY5.5⁺, Ly6G FITC⁺), eosinophils (c-Kit APC⁻, Siglec-F PE⁺), and alternatively activated (M2) macrophages (F4/80 APC⁺, CD206 Alexa Fluor 488⁺). The mean and se is shown for each treatment group along with the exact p values and the number (N) of individual mice, 4 or 5/treatment group, which varied with availability of mice.. No outliers were removed from analyses and measurements were taken from distinct samples. Statistical tests are as described in Fig. 1. All experiments were performed two times with similar results.

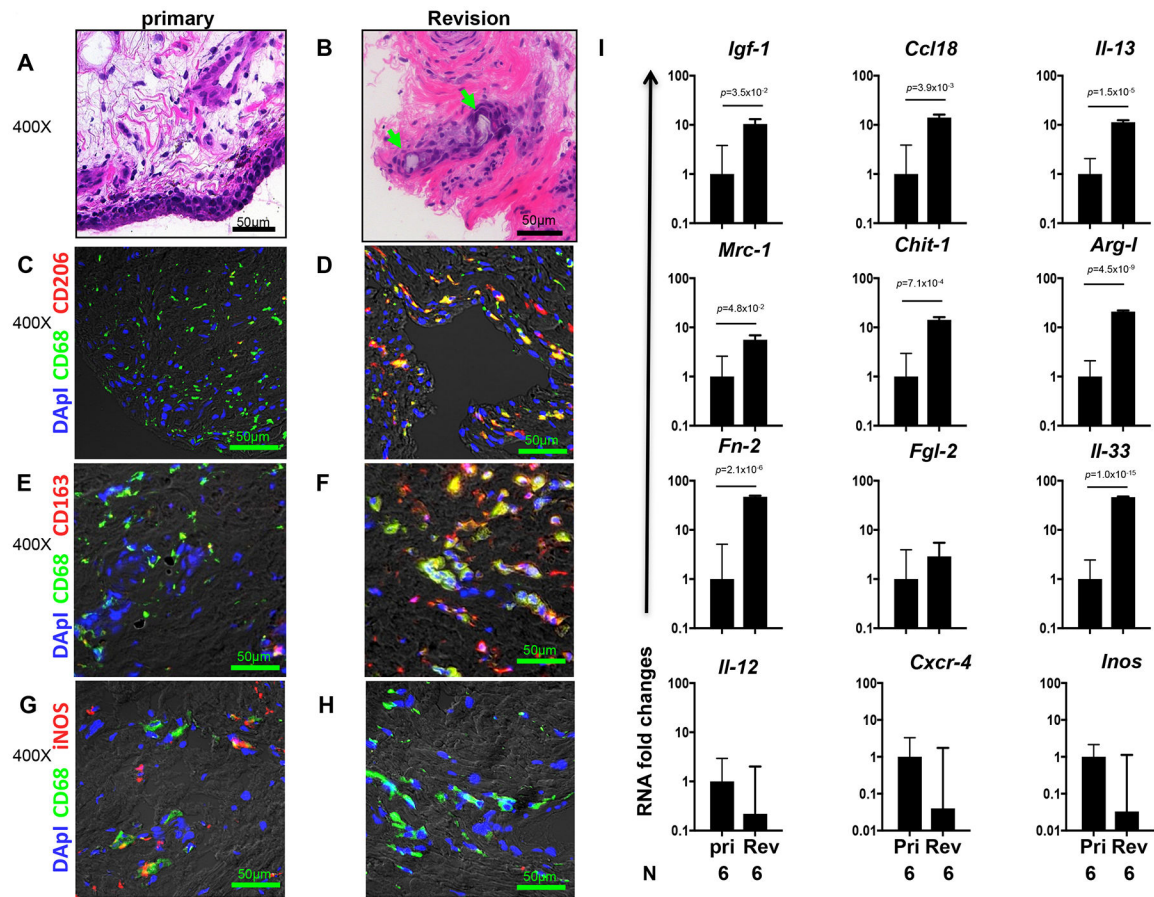


Fig 6: Increased M2 macrophage markers detected in periprosthetic tissues

Histological analysis of infiltrate surrounding wear debris in revision joint replacement or control primary implant. (A-B) Slides were stained with H&E and infiltrates surrounding polyethylene particles identified by polarized light microscopy (indicated by green arrows). Frozen sections were dual stained to identify M2 macrophages using anti-CD68 in combination with either anti-CD206 (C, D) or anti-CD163 (E, F). M1 macrophages were identified using anti-CD68 and anti-iNOS (G, H). All photos were digitally imaged at 400 \times and scale bar of 50 μ m size is shown in each image. Quantitative real-time PCR showed significant increases in gene expression of alternatively activated (M2) macrophage markers, type 2 cytokines, and associated wound healing related genes in joint tissue of revision patients compared to primary patients (I). The mean and se is shown for each marker along with the exact p value and number (N) of individual clinical samples (N=6). GraphPad Prism software was used to perform unpaired two sided T test. Pri = Primary arthroplasty; Rev = Revision arthroplasty.